ARTICLE IN PRESS

Available online at www.sciencedirect.com

ScienceDirect

Advances in Space Research xxx (2020) xxx–xxx

ADVANCES IN SPACE RESEARCH (a COSPAR publication)

www.elsevier.com/locate/asr

The effects of ocean temperature gradients on bigeye tuna (*Thunnus obesus*) distribution in the equatorial eastern Pacific Ocean

LiNa Cai [a,b], LiLi Xu [c], DanLing Tang [d,*], WeiZeng Shao [a], Yu Liu [a], JunCheng Zuo [a], QiYan Ji [a]

[a] *Zhejiang Ocean University, Zhoushan, Zhejiang 316004, China*

[b] *Key Laboratory of Informalization of Habitat Monitoring and Fishery Resource Conservation Research in the East China Sea of Zhejiang Province, China*

[c] *Beijing Aerospace Titan Technology Co., Ltd., Beijing 100070, China*

[d] *Guangdong Key Laboratory of Ocean Remote Sensing (LORS), Southern Marine Science and Engineering Guangdong Laboratory (Guangzhou) State Key Laboratory of Tropical Oceanography (LTO), South China Sea Institute of Oceanology, Chinese Academy of Sciences, Guangzhou 510301, China*

Received 8 September 2019; received in revised form 21 March 2020; accepted 25 March 2020

Abstract

The water temperature at 100–300 m depth layer impact on bigeye tuna distribution has been studied from data collected by 15 fishery survey vessels, surveying every day, in the Equatorial Pacific Ocean from February to March and June to September 2010. The in situ ocean temperature measurements at four depths (100, 150, 200, and 300 m), satellite data and TAO/TRITON moored buoy data were also augmented in this study. The results reveal stereoscopic temperature factors for the prediction of tuna fishing ground: horizontal temperature gradient (HTG), vertical temperature gradient (VTG) in the 100–300 m layer. Maximal catches were observed where (1) vertically there has a strong subsurface temperature front in the 150–200 m layer, with horizontal temperature gradient up to near 0.020 °C/km; (2) there have vertical temperature gradient between −0.088 and −0.066 °C/m. Meanwhile, the monthly tuna fishery catches decrease with the synchronized reduction of 20 °C isotherm depth in the ocean.

Keywords: Pacific Ocean; Bigeye tuna; Temperature gradient; Ocean fronts

1. Introduction

Bigeye tuna, a marine migratory fish with instantaneous swimming speed of up to 160 km/h (Leroy et al., 2007; Evans et al., 2008), inhabits the Pacific, Indian, and Atlantic Ocean (Chiang et al., 2008) and is one of the most economically important pelagic fishes in the world (Musyl et al., 2010). Previous studies have revealed close relationships between bigeye tuna distribution and marine environmental factors, e.g., temperature (Yang et al., 2015), salinity (Song et al., 2004), sea surface height (Lumban-Gaol et al., 2015), chlorophyll-a concentration (Song et al., 2015) and so on. Among them, sea water temperature has great significance in the formation of bigeye tuna fishing grounds (Song et al., 2009). Bigeye tuna actives vertically from the 0–100 m layer (Dagorn et al., 2000), to about 250 m' deep. The bigeye tuna migrates vertically every day, ascending to the upper layer at night and descending during the day. During the daytime, bigeye tuna dives below the thermocline for feeding on deep scattering layer (DSL) organisms (Howell et al., 2010; Matsumoto et al., 2013). The high-speed movements of

* Corresponding author.
E-mail address: lingzistdl@126.com (D. Tang).

https://doi.org/10.1016/j.asr.2020.03.030
0273-1177/

Please cite this article as: L. Cai, L. Xu, D. Tang et al., The effects of ocean temperature gradients on bigeye tuna (*Thunnus obesus*) distribution in the equatorial eastern Pacific Ocean, Advances in Space Research, https://doi.org/10.1016/j.asr.2020.03.030

bigeye tuna, especially over vertical distance (Lam et al., 2014), are thought to reduce the correlation between bigeye tuna fishing locations and sea surface temperature, SST (Song et al., 2009). Meanwhile, the spatial distribution of thermocline directly affects the formation of oceanic tuna fishing grounds (Yang et al., 2015; Li et al., 2012).

Bigeye tuna has a life habit of vertical movement. Therefore, it is of great significance to study the vertical variations of environmental factors (especially temperature gradient) relevant to the bigeye tuna diurnal vertical migrations.

In terms of temperature, which layer of seawater with a depth of 100 m, 150 m, 200 m, 300 m will have a greater impact on the distribution of bigeye tuna? Based on bigeye tuna fishery catches, moored measurements, satellite data and Argo float data in the equatorial Pacific Ocean, we analyzed the relationship between the bigeye tuna catch and the water temperature in each layer (including the horizontal temperature gradient in each layer) and the corresponding relationship between the vertical temperature gradient and the catch.

The paper is structured as follows. Section 2 describes data sets and data processing. Section 3 describes: (1) The effects of both horizontal water temperature gradients at different depths and vertical temperature gradient on the bigeye tuna catch; (2) The relationship between bigeye tuna catch and depth of the 20 °C isotherm. (3) The relationship between bigeye tuna catch and other factors. Discussion and Conclusions are summarized in Section 4 and Section 5.

2. Data and method

2.1. Study area

The study area in the equatorial eastern Pacific Ocean (125–160°W, 5°N–15°S; Fig. 1) is characterized by warm waters (SST > 25 °C) flowing westward (Wang and Hu, 2006). There are three main tuna species: yellowfin tuna, bigeye tuna and longfin tuna. Among them, bigeye tuna and yellowfin tuna are active largely in the 0–100 m layer (Dagorn et al., 2000), to much deeper, diving down to around 250 m; while longfin tuna is active below the thermocline, down to 600 m (Laurs et al., 1984). The bigeye tuna migrates vertically every day, ascending to the upper layer at night and descending below the thermocline during the day. The locations of the bigeye tuna catches are shown in Fig. 1.

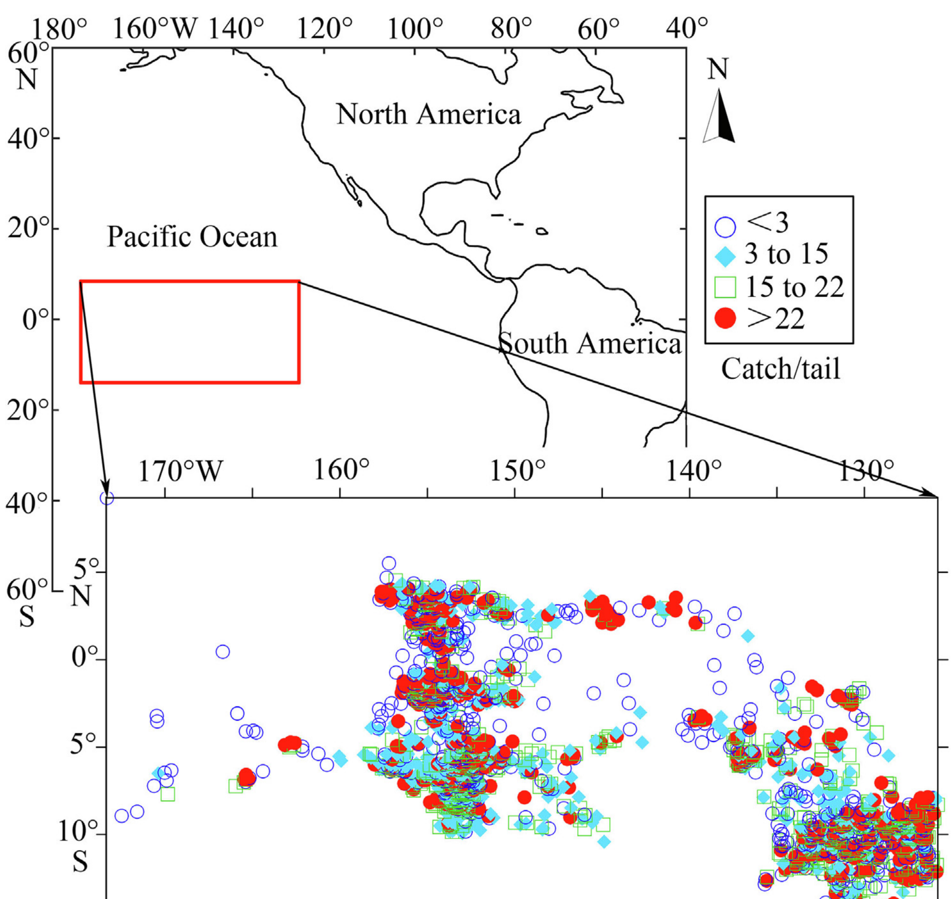

Fig. 1. Study area (red rectangle) and locations of bigeye tuna fishery catches (colored symbols). (For interpretation of the references to color in this figure legend, the reader is referred to the web version of this article.)

Please cite this article as: L. Cai, L. Xu, D. Tang et al., The effects of ocean temperature gradients on bigeye tuna (*Thunnus obesus*) distribution in the equatorial eastern Pacific Ocean, Advances in Space Research, https://doi.org/10.1016/j.asr.2020.03.030

2.2. Data

The in-situ data set consists of data collected by 15 fishery survey vessels (Table 1) (every day) in February to March and June to September 2010, including bigeye tuna catch, in-situ sea surface height (SSH) and vertical water temperature at 100, 150, 200, and 300 m depth. The tonnage of each fishing vessel is 700 tons. The method of catching tuna is longline fishing. The process of longline fishing in this study is: a main rope is released from the fishing vessel to the ocean. There are a certain number of supporting ropes and floats on the main rope at a certain distance. With the buoyancy of the floats, the bait of the supporting rope (one end with bait, such as frozen saury, mackerel, sardines, squid and so on) is stable on the hook. In the ocean, the hook depth is mainly between 120 and 300 m. Fish bait (or bait) is used to induce tuna to bite hook, so as to achieve the purpose of fishing. The total length of the main rope is 130–150 km. Sixteen support ropes are hung between the two floats at 867 m. The length of the float rope is 40 m, the length of the supporting rope is 57 m (Fig. 2), and the average speed of fishing vessel is 10.02 kn.

Table 1
Survey areas of fishery survey vessels.

Vessel number	Survey area
1	136.133°–162.817°W, 2.667°N–6.033°S
2	127.767°–155.533°W, 3.600°N–13.617°S
3	146.850°–158.233°W, 4.383°N–9.700°S
4	126.633°–152.483°W, 3.567°N–13.917°S
5	150.650°–157.600°W, 3.417°N–9.700°S
6	144.900°–158.450°W, 3.700°N–10.400°S
7	125.883°–153.617°W, 3.450°N–14.000°S
8	125.817°–151.000°W, 3.650°N–14.150°S
9	150.967°–157.617°W, 4.367°N–9.833°S
10	146.267°–158.400°W, 4.550°N–9.167°S
11	127.317°–155.917°W, 3.283°N–13.867°S
12	151.100°–158.183°W, 4.717°N–9.900°S
13	125.917°–165.867°W, 4.050°N–10.800°S
14	127.217°–165.867°W, 3.717°N–11.367°S
15	134.267°–153.933°W, 3.333°N–9.650°S

The monthly mean chlorophyll-a concentration and monthly mean SST from February to September 2010 (based on MODIS Aqua data) were downloaded from the NASA Ocean Color Web site (http://oceancolor.gsfc.nasa.gov).

The daily SST data from February to September 2010 (based on Group for High Resolution Sea Surface Temperature data) was download from the Asia-pacific data research center (http://apdrc.soest.hawaii.edu/data/data.php).

Mooring buoy data obtained from the Pacific Tropical Atmospheric Marine Mooring Buoy System TAO/TRITON included vertical profiles of water temperature down to 500 m depth (http://www.pmel.noaa.gov/tao/data_deliv/frames/main.html).

2.3. Data processing

2.3.1. In situ data

Maps of temperature at four pre-selected depths (100, 150, 200, and 300 m) have been generated by spatial and

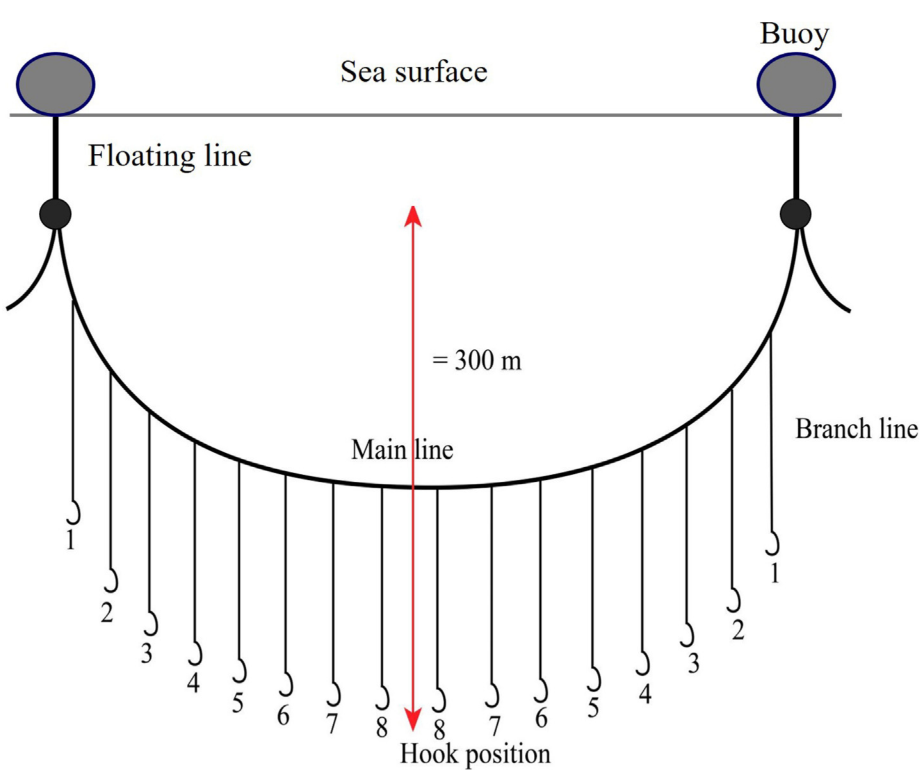

Fig. 2. Structure of bigeye tuna fishing gear.

Please cite this article as: L. Cai, L. Xu, D. Tang et al., The effects of ocean temperature gradients on bigeye tuna (*Thunnus obesus*) distribution in the equatorial eastern Pacific Ocean, Advances in Space Research, https://doi.org/10.1016/j.asr.2020.03.030

temporal interpolation of the in situ data. The interpolation method used here is Kriging. Kriging is an effective geostatistical gridding method that can represent the trends implied in the data (Oliver and Webster, 1990) more accurately. Horizontal temperature gradient has been computed at each depth. A strong temperature front (described below) has been revealed in the 150–200 m layer, defined as a locus of the maximal horizontal temperature gradient (Belkin et al, 2009; Liu et al, 2018). Relationship between the temperature at four selected depths and the collocated tuna catches have been analyzed using the IBM SPSS software.

In this paper, the catch rate, CPUE (catch per unit effort) united in tail·1000 hooks^{-1}, is counted on a $5° \times 5°$ grid. CPUE is calculated by following Eq. (1),

$$CPUE_{(m,n)} = \frac{\sum C_{(m,n,i)} \cdot 1000}{\sum H_{(m,n,i)}} \quad (1)$$

where C is catch, H is the number of hooks, $CPUE_{(m,n)}$, $C_{(m,n,i)}$, $H_{(m,n,i)}$ are the average CPUE, the ith catch and the ith number of hooks of the nth calculation unit in the mth latitude upward. Both CPUE and catch represent catches.

The CPUE in this paper is based on the average catch per 1000 hooks per unit area calculated by catch with 5 * 5 (5 longitudes * 5 latitudes) as the unit surface (see Formula 1), that is, an unit area corresponds to a CPUE value. There may be n catch values of measuring points in a unit area, but there is only one CPUE value. The fishing intensity of each fishing location is the same, that is, the same type of fishing boat, the same way of operation, the same fishing time.

Although both CPUE and catch represent catches, they are applicable to different situations. CPUE can macroscopically reflect the distribution of bigeye tuna in a large area. A CPUE value can correspond to a unit area, but a CPUE value can't correspond to the point data such as in situ measured sea surface height, temperature and other data of a fishing location. There is no one-to-one correspondence between the data of unit area and the data of a point. However, the catch (point data) of a fishing location can correspond to the point data of synchronous measured temperature, sea level height and other data of this fishing location

The change intensity of vertical temperature (vertical temperature gradient) has been analyzed using the in-situ measurements of vertical temperature. The thermocline appears mostly at the depth of 100–300 m in study area. In addition, in the depth range of 100–300 m, water temperature decreases with the increase of water depth. Therefore, in order to reveal the vertical change of temperature on bigeye tuna catch we computed vertical temperature gradient (Belkin et al., 2009) between 100 and 300 m depth using formula (2).

$$G_{(j)} = \frac{T_{300(j)} - T_{100(j)}}{200} \quad (2)$$

where $G_{(j)}$, $T_{300(j)}$, $T_{100(j)}$ are vertical temperature gradient, temperature at 300 m depth, and temperature at 100 m depth at the jth measurement location.

2.3.2. Satellite data

To further reveal the possible factors affecting the distribution of bigeye tuna, sea surface chlorophyll-a concentration (monthly composites with 4 km resolution) and monthly mean SST were derived from the Moderate Resolution Imaging Spectroradiometer (MODIS) data onboard the NASA Aqua satellite which was launched in 1999. The data were downloaded from the Distributed Active Archive Centre (DAAC) of NASA (http://oceancolor.gsfc.nasa.gov). The daily SST were download from the Asia-pacific data research center (http://apdrc.soest.hawaii.edu/data/data.php)

3. Results

3.1. Spatial distribution of catch in the study area

The 15 survey vessels conducted daily measurements in the study area for 6 months. During this time, we got more than 2,000 bigeye tuna catches, from which CPUE values were also obtained.

The bigeye tuna catches in the study area are mainly concentrated in two regions (Fig. 1), with the highest catches distributed around150°–160°W, 5°N–10°S and 125°–135°W, 5°–12°S. The spacial distribution of CPUE values is consistent with that of the bigeye tuna catches. There are many prior studies focusing on the distribution of bigeye tuna in the eastern Pacific Ocean, but few of them are about the distribution of bigeye tuna in the two regions mentioned above in this paper.

3.2. Relationship between catch and water temperature at various depths

The relationship between catch and water temperature is revealed by histogram of catch in 0.1 °C intervals at various depths (Fig. 3).

These distributions are approximately normal at 100 m and at 300 m depth. At 150 m depth, the catch distribution is quasi-normal and has a well-defined mode at 22 °C. At 200 m depth, the catch distribution is almost uniform with respect to water temperature, the later varying widely across a 6.5 °C range, from 12.5 °C up to 19 °C. The abnormal distribution of catches with respect to water temperature at 200 m depth is caused by a subsurface front described below.

The results of normal test and statistical analysis of bigeye tuna catches and temperature at different water depths are shown in Table 2.

From the analysis above, we can see that in high bigeye tuna catch area, the corresponding temperature range for bigeye tuna at depths of 100 m, 150 m, 200 m, 300 m are

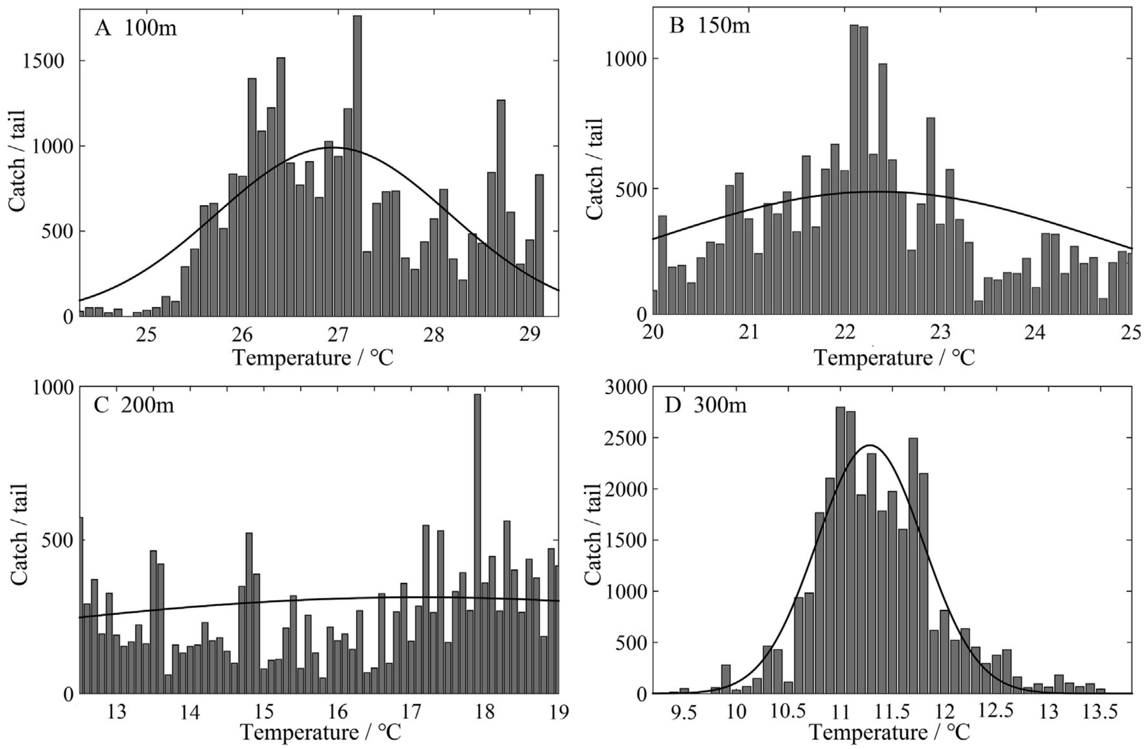

Fig. 3. Bigeye tuna catch as a function of water temperature at various depths.

Table 2
Statistical analysis of bigeye tuna catch and temperature of each depth.

Test of Normality				Confidence Interval of Catches with 95% Confidence Level (tail)	
Depth (m)	Kolmogorov-Smirnov				
	Statistic	df	Sig.	Minimum	Maximum
0	0.097	55	0.200	18764.89	28219.58
50	0.132	43	0.056	23697.28	36399.14
100	0.242	110	0.000	8737.18	14755.06
150	0.159	151	0.000	7175.11	9930.10
200	0.113	117	0.001	9576.32	12510.39
300	0.237	46	0.000	17638.41	38538.67

25.3–29.0 °C, 19.6–25.6 °C, 11.5–22.0 °C, 10.4–12.3 °C respectively.

The monthly mean SST maps from MODIS show that during February to September, the SST in the study area decreases from 33.5 °C to 26.5 °C (Fig. 4). The bigeye tuna catches also show the decrease trend accordingly (Fig. 5). Because of the vertical movement of bigeye tuna, the influence of SST on the catch of bigeye tuna is not direct. Therefore, the change trend of bigeye tuna catch is mainly induced by the seasonal variation.

3.3. Relationship between CPUE and horizontal temperature gradient at various depths

Temperature maps (Fig. 6) reveal a distinct temperature front in the 150–200 m layer. The maximal horizontal temperature gradients across this front are 0.021 °C/km at 150 m depth and 0.019 °C/km at 200 m depth. High catches are concentrated in the vicinity of this front (Fig. 6).

3.4. Relationship between CPUE and vertical temperature gradient

Tuna is known to prefer high-gradient zones, both in horizontal plane (fronts) and in vertical plane (thermocline). In fact, thermocline is a quasi-horizontal front, a locus of maximal vertical gradient. In the study area, the observed frequency distribution of catches with respect to vertical gradient (Fig. 7) has a well-defined mode at −0.077 °C/m. Statistical analysis of the bigeye tuna catch and the vertical temperature gradient shows that the confidence interval of the 95% confidence level was 342.30–926.57 tails. The bulk of catches correspond to the vertical temperature gradient range of −0.066 °C/m to −0.088 °C/m.

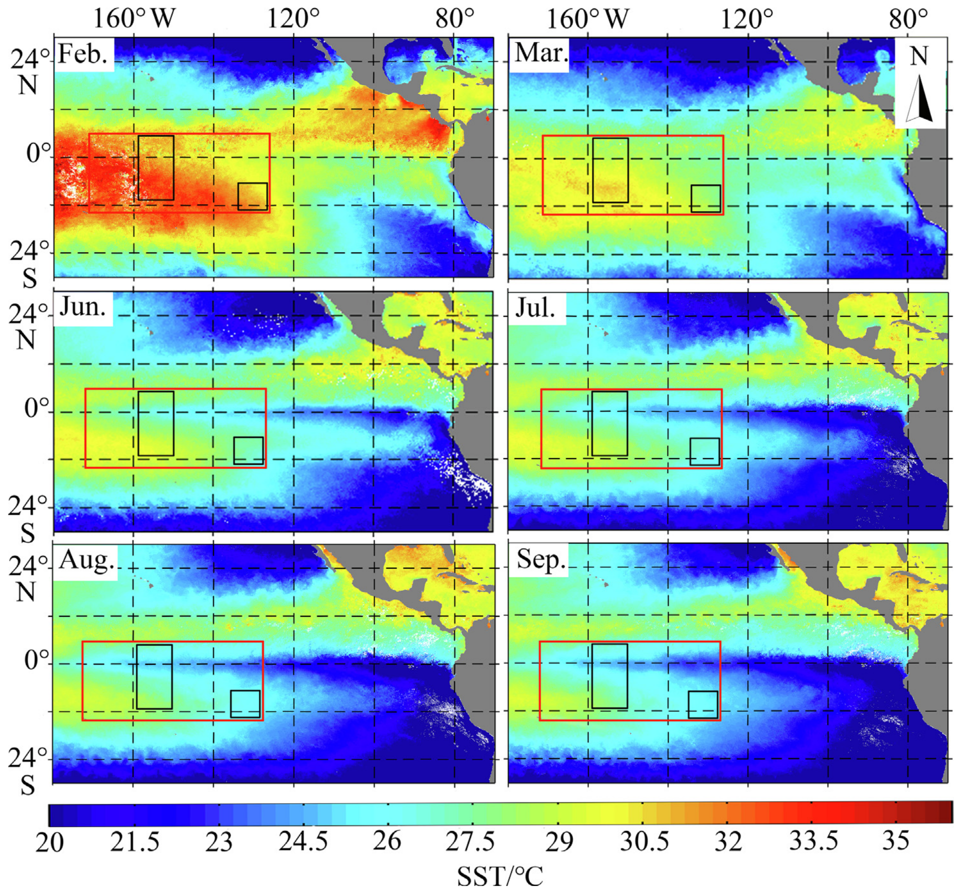

Fig. 4. Monthly mean SST maps in 2010. The red box is the study area; the black boxes are high catch areas. (For interpretation of the references to color in this figure legend, the reader is referred to the web version of this article.)

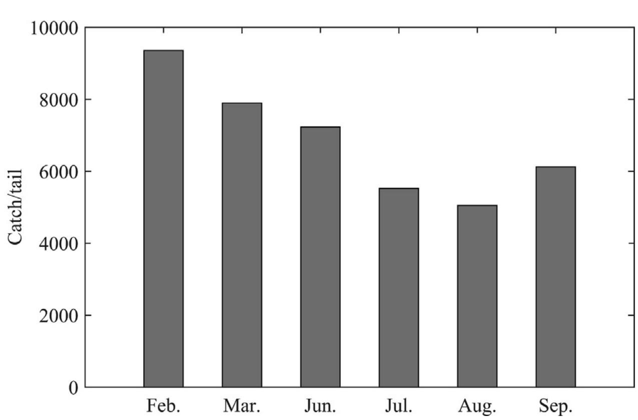

Fig. 5. Bigeye tuna catch as a function of month.

3.5. Relationship between CPUE and depth of the 20 °C isotherm

The 20 °C isotherm coincides with the thermocline axis in the study area. This isotherm has been used in many studies to map the thermocline axis. Vertical sections of water temperature in the study area reveal a broad thermocline between 12–13 °C and 28–29 °C, with the 20 °C isotherm approximating the thermocline axis, where all high catches are observed (Fig. 8). Thus, the depth of the 20 °C isotherm is a reliable predictor of high catches.

The depths of isotherm at 20 °C in high bigeye tuna CPUE locations corresponding to 2°S, 5°S and 8°S are mainly concentrated in the range of 60–175 m, 65–180 m and 130–210 m respectively (marked as red ovals in Fig. 8-A-1, B-1, C-1). The depth of isotherm at 20 °C increases with increasing latitude in study area. The depth of isotherm at 20 °C decreases from February to September, the fishery catches are also decreasing correspondingly. Meanwhile, in high bigeye tuna catch area, in the depth range of the isotherm at 20 °C, the temperature anomaly is evident (Fig. 8A-2, B-2, C-2), i.e., temperature anomalies are generally high at 1–4 °C, and in August and September there are individual abnormalities of 4–5 °C.

3.6. Relationship between CPUE and Chlorophyll-a concentration

The maps of long-term monthly mean chlorophyll-a concentration in the study area are shown in Fig. 9.

The chlorophyll-a concentration in high bigeye tuna catch area is generally very low (Fig. 9), with the value being largely around 0.2 $mg{\cdot}m^{-3}$ and 0.1 $mg{\cdot}m^{-3}$. The monthly average chlorophyll-a concentration in February

Please cite this article as: L. Cai, L. Xu, D. Tang et al., The effects of ocean temperature gradients on bigeye tuna (*Thunnus obesus*) distribution in the equatorial eastern Pacific Ocean, Advances in Space Research, https://doi.org/10.1016/j.asr.2020.03.030

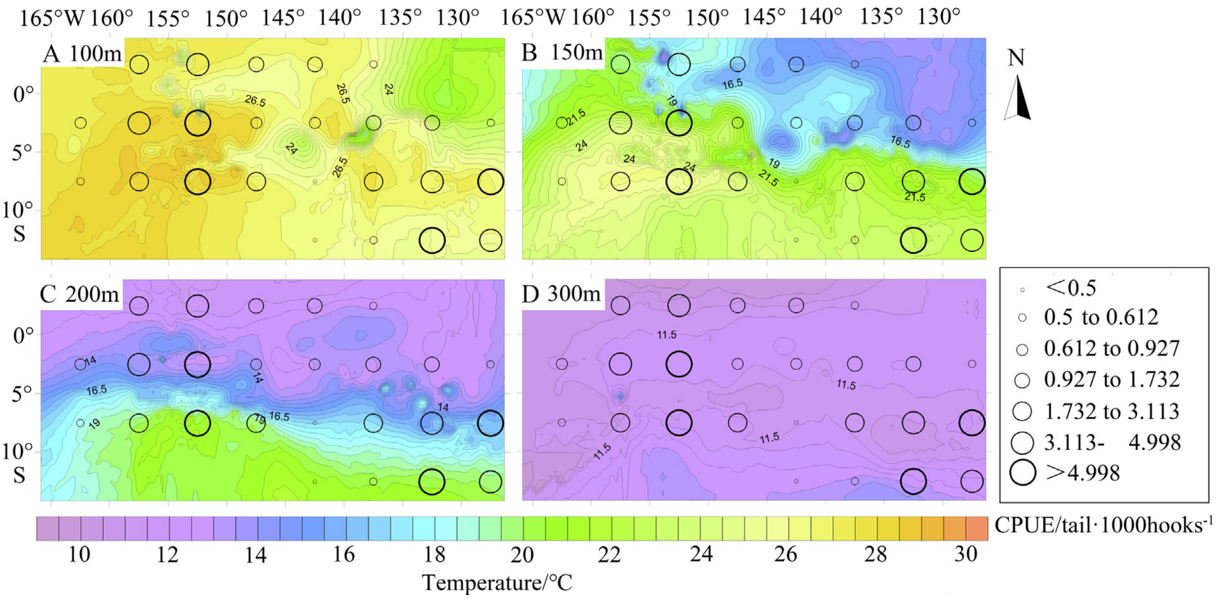

Fig. 6. CPUE (circles) locations and temperature (colors and isotherms) at various depth.

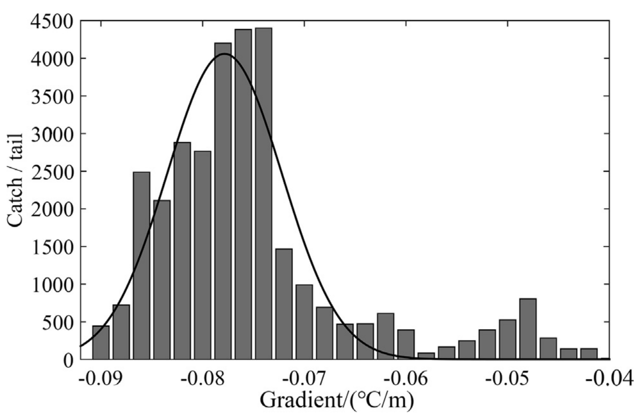

Fig. 7. Bigeye tuna catch as a function of vertical temperature gradient.

and March is lower than in June through September, with the maximum of around 0.7 mg·m^{-3} being attained in June. The prey of bigeye tuna is small fish, not phytoplankton/chlorophyll-a. Therefore, sea surface chlorophyll-a concentration in the study area showed no direct correlation with bigeye tuna catch with the correlation being −0.48.

3.7. Relationship between CPUE and SSH

In order to visualize a possible relationship between tuna catches and SSH, the catches have been superimposed onto a map of SSH generated from in situ data (Fig. 10). The confidence interval for catches at the 95% confidence level is 8424.03–30870.03 tails. It can be seen from Fig. 10 that the sea surface heights at high catch locations (CPUE > 1.8) are concentrated in the range of 40–65 cm. The frequency histogram of catches vs. SSH (Fig. 11) shows that the catches are higher in the SSH range of 40–55 cm, peaking at SSH of 44 cm. Our results are consistent with the findings in previous studies (Howell and Kobayashi, 2006; Lehodey, 1997).

4. Discussions

4.1. Water temperature

Temperature is one of the most important environmental factors affecting the activities of bigeye tuna and it is of great significance in the formation of tuna fishing grounds (Song et al., 2009). The changes of water temperature affect the distribution, migration and clustering activities of fish (Brill et al., 1994). Studying the relationship between bigeye tuna distribution and the temperature factors, especially the temperature gradient, can effectively help us make fishery ground prediction.

Bigeye tuna is common in the tropical waters of high temperature, and the SST in high-yield fishing areas is relatively high (Dagorn et al., 2000; Bertrand et al., 2002). The average SST in the main fishing grounds of longline bigeye tuna in the Pacific Ocean is largely around 24–29 °C (Fan et al., 2008). The monthly bigeye tuna catches in the study area show a same downward trend as the monthly mean SST, with the highest in February and the lowest in August (Fig. 5).

Tuna dives under the thermocline in the daytime to feed on deep-sea scattering layer (DSL) organisms, and swims back to the upper mixed layer at night (Dagorn et al., 2000; Howell et al., 2010). Therefore, the depth of thermocline directly affects the vertical distribution of tuna (Houssard et al., 2017) and is essential in tuna fishery forecasting. Typically, the depth of thermocline in the Pacific Ocean is expressed by the depth of 20 °C isotherm (Zagaglia et al., 2004).

Please cite this article as: L. Cai, L. Xu, D. Tang et al., The effects of ocean temperature gradients on bigeye tuna (*Thunnus obesus*) distribution in the equatorial eastern Pacific Ocean, Advances in Space Research, https://doi.org/10.1016/j.asr.2020.03.030

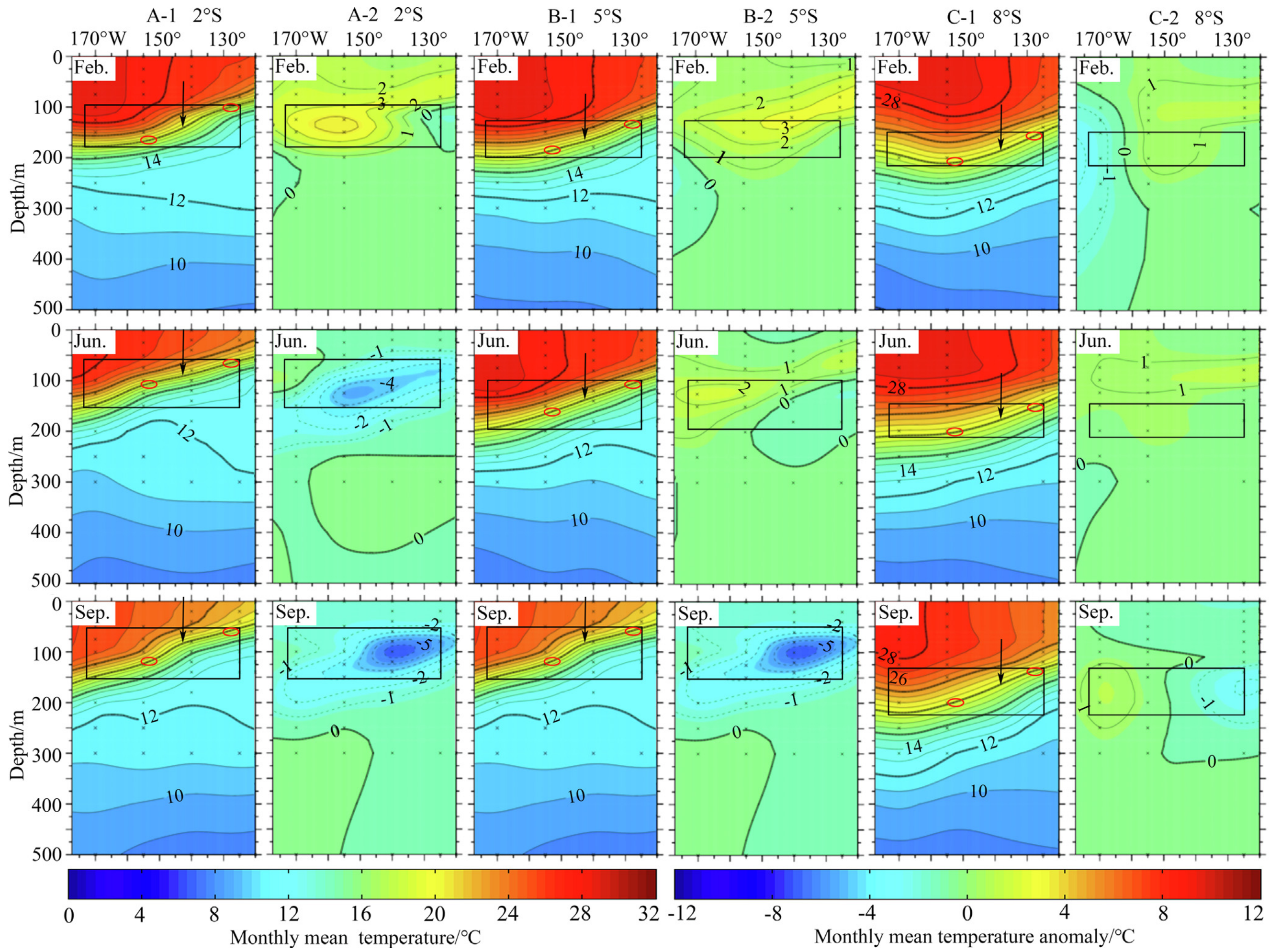

Fig. 8. Monthly mean water temperature in 2010 as a function of depth and longitude at 2°S, 5°S, and 8°S. The black rectangle is the depth range of the 20 °C isotherm in the study area; the black arrows point to the 20 °C isotherms; the red ellipses mark the 20 °C isotherm in the high catch areas. Heavy contours of temperature are drawn every 4 °C. (For interpretation of the references to color in this figure legend, the reader is referred to the web version of this article.)

Meanwhile, in high tuna catch area, the subsurface temperature front, with horizontal temperature gradient of 019–0.020 °C/km, at the depth of 150–200 m (HTG) is obvious. Near the temperature fronts, different currents meet carrying nutrients that allow phytoplankton to thrive. As a result, many zooplankton and marine fish with different ecological habits often gather near the front to feed, lay eggs or migrate. These fish provide a food source for the bigeye tuna. Meanwhile, the vertical temperature gradient across the thermocline in high catch areas is mainly in the range of −0.088 to −0.066 °C/m. As there are few studies on the influence of vertical temperature gradient of 100–300 m depth on the distribution of bigeye tuna, the innovation of this paper is to reveal the relation between the distribution of bigeye tuna and the vertical temperature gradient. We found that, the vertical temperature gradient across the thermocline in high catch areas is mainly in the range of −0.088 to −0.066 °C/m. This temperature gradient is suitable for the behavior of bigeye tuna, and the mechanism needs further study.

Therefore, the horizontal and vertical temperature gradients together with the depth of 20 °C isotherm can be used as reliable predictors in tuna fishing forecasting. These temperature factors can be defined as stereoscopic temperature factors for the prediction of tuna fishing ground.

4.2. Chlorophyll-a concentration and SSH

Chlorophyll-a concentration has a significant effect on the distribution of fishing grounds (Anand et al., 2005; Song and Zhou, 2010; Song et al., 2015). Prior studies have found that the average chlorophyll-a concentration in the entire euphotic layer is positively correlated with the catch rate of bigeye tuna (Song and Zhou, 2010). However, chlorophyll-a concentration has no obvious effect on the distribution of bigeye tuna in the study area. Meanwhile, the vertical motion of bigeye tuna reduces the dependence of tuna on sea surface features.

Although the sea surface height (SSH) per se does not directly affect the bigeye tuna's activity, it is found that

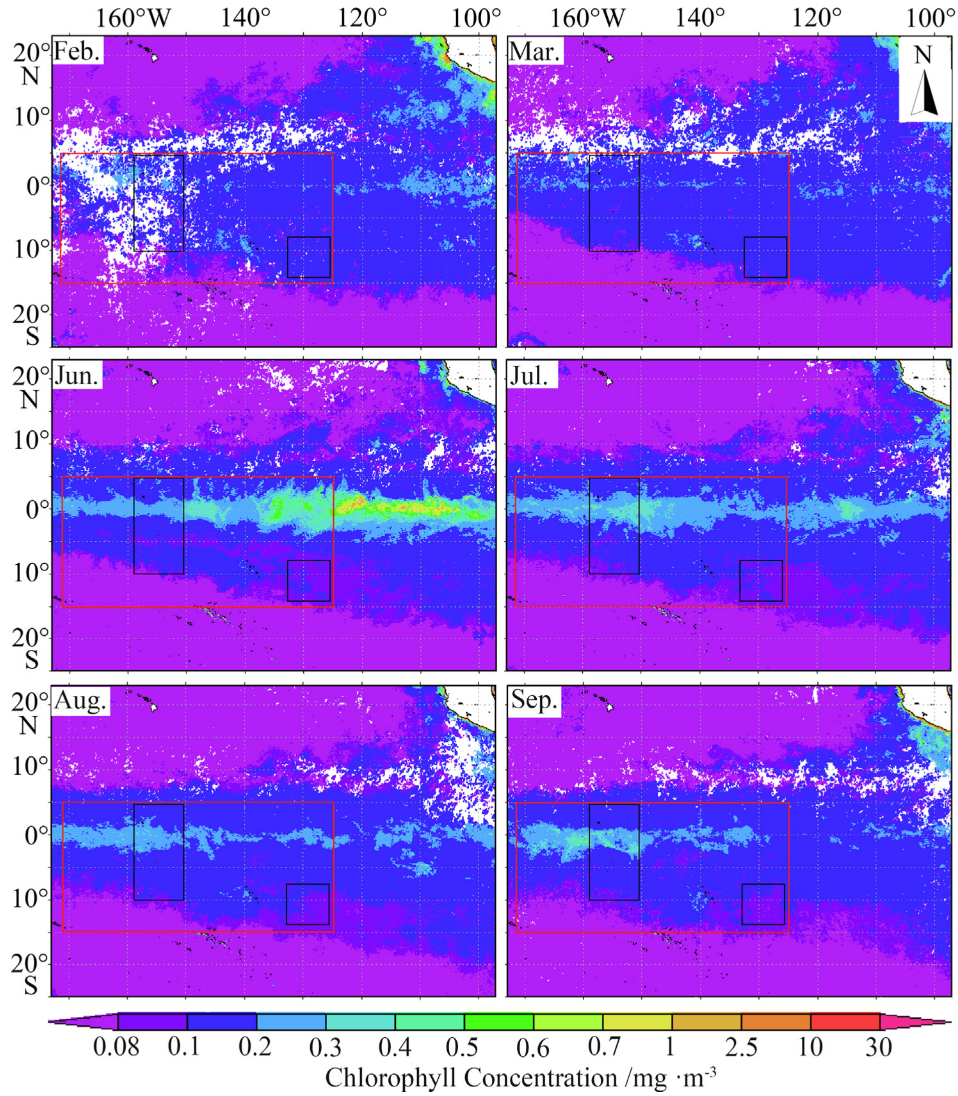

Fig. 9. Monthly mean chlorophyll-a concentration maps in 2010. The red box is the study area; the black boxes are high catch areas. (For interpretation of the references to color in this figure legend, the reader is referred to the web version of this article.)

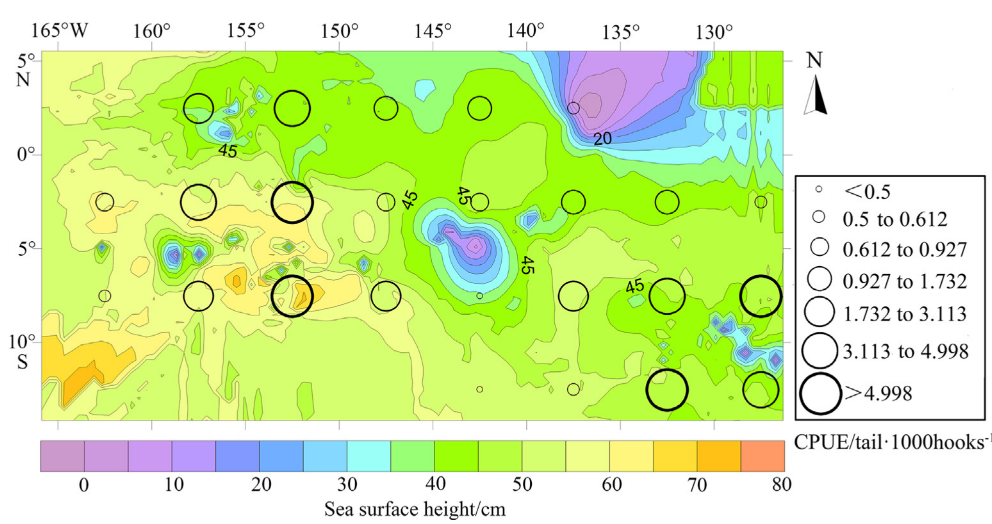

Fig. 10. Sea surface height (color and contours) and CPUE (circles).

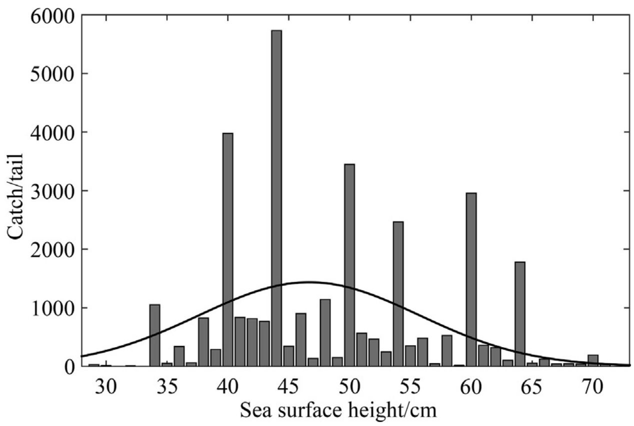

Fig. 11. Bigeye tuna catch as a function of SSH.

the sea area with SSH of 40–80 cm accounts for >91% of the total catch in this area (Howell and Kobayashi, 2006; Lehodey, 1997), which showing the correlation between the SSH distribution and the observed distribution of bigeye tuna (Howell and Kobayashi, 2006). Our in situ data also indicated that the sea surface heights at high catch locations (CPUE > 1.8) are concentrated in the range of 40–65 cm.

Many reasons can induce the change of SSH. In equator area, due to the prevailing easterly winds in the equatorial Pacific Ocean, the warm surface water is transported to the Western Pacific Ocean, resulting in the SSH in the west being higher than the east (Lehodey, 1997; Evans et al., 2013; Abascala et al., 2018) by 40 cm. Eddies can also lead the change of SSH and other ocean environmental factors (Howell and Kobayashi, 2006; Liu et al., 2012; Sun et al., 2017; Sun et al., 2018).

From daily SST (Fig. 12) we can see clearly that there exist a lot of warm eddies in study area (here we take the daily SST of the end of the month during the period for data acquisition as examples). The eddies are very obvious in study area from May to September. Generally, due to the convergency of surrounding water, warm-core eddy can increase the SSH and deepen the thermocline (Liu et al., 2012). Prior study found that the development of eddies contributes to the increase of bigeye tuna and that SSH distribution is correlated with the observed distribution of bigeye (Lumban-Gaol et al., 2015).

4.3. Other reasons contributing to the distribution of bigeye tuna

Bigeye tuna occupies water masses of 2.7–28.2 °C and depths of 0–1280 m, with deeper depths in the day time (daily mean ± standard deviation: 196 ± 92 m) than at night time (45 ± 29 m) (Lam et al., 2014). The vertical movements of bigeye tuna are related to the thermoregulation and the movements change with time of day, season, and body size.

Bigeye tuna can grow up to 98 in. (or 8 feet), in length. Maximal weight of individuals probably exceeds 180 kg, with the all-tackle angling record standing at 178 kg and fish size increased with deeper depths. Seasonal change of vertical thermal structure of the ocean influences tuna's

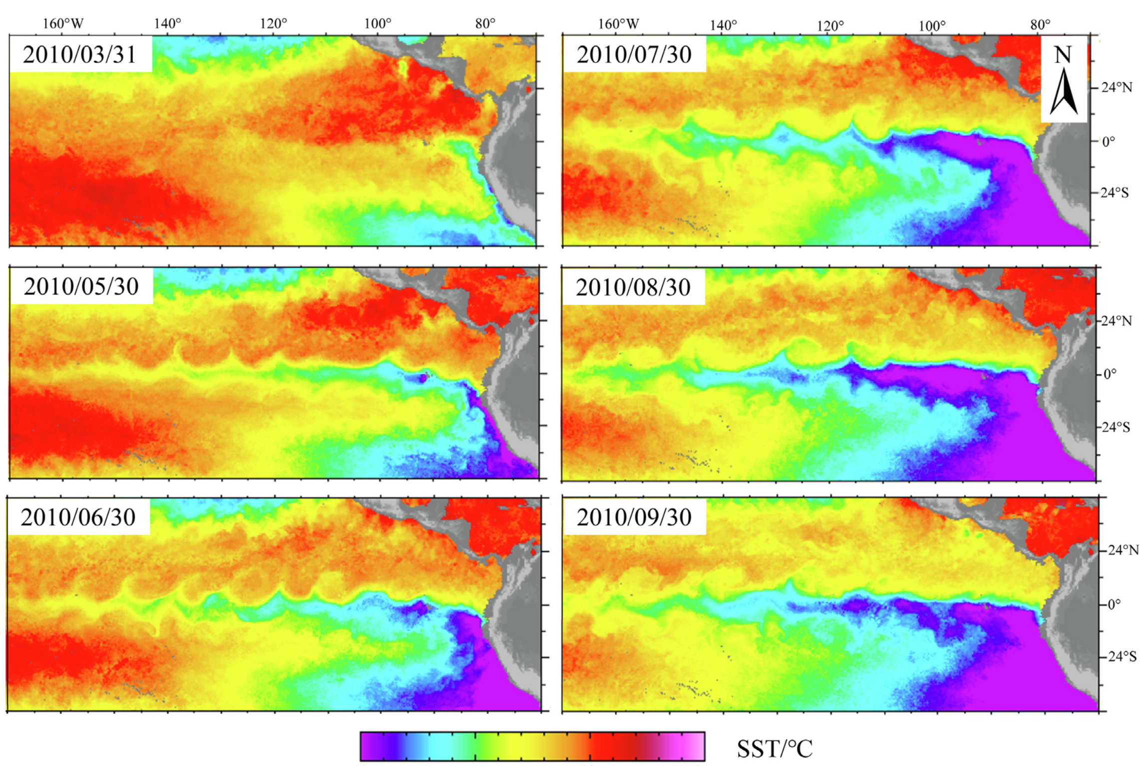

Fig. 12. Daily SST maps in 2010.

ascent behavior, i.e. from cold month to warm month, bigeye tuna makes fewer ascents to less shallow waters. In addition, as body size increases, fish will remain deeper for longer periods (Fuller et al., 2015). Meanwhile, there is a significant positive correlation between the proportion of time fish exhibits characteristic behavior and fish length, and significant negative correlations between the proportion of time bigeye tuna exhibit associative and other behavior with fish length (Jean-Rene and Meyers, 1987).

The seasonal variations in the upper boundary temperature and depth of thermocline in the central fishing grounds are significant (Yang et al., 2015). Prior study found that seasonal monsoon influences the distribution of bigeye tuna by an offshore Ekman transport (Lumban-Gaol et al., 2015; Syamsuddin et al., 2016). Seasonal temperature variations are most pronounced at the surface and mixed layer, influencing bigeye tuna nighttime occupancy at shallow depths (Lam et al., 2014).

The seasonal cycles of the tropical area were also estimated, in prior study, as well as a simple El Nino Southern Oscillation (ENSO) cycle and found the change of near-equatorial and subthermocline currents (Hino et al., 2019). The analysis of variability in depth of the 20 °C isotherm during 1979 to 1983 at selected locations shows obvious interannual signals. Significant annual change appears in observed and modeled of the topography of 2O °C isotherm in the tropical Pacific topography (Cravatte et al., 2017).

There exist monthly, seasonal and annual variations of marine environmental factors, therefore inducing monthly, seasonal annual variations both in the horizontal and vertical distribution of tuna. The interannual variation of tuna distribution will become more obvious in special years, such as El Nino year and La Nina year (Mysak, 1986).

5. Conclusion

We investigated the effects of ocean temperature, especially temperature gradient, on bigeye tuna (*Thunnus obesus*) distribution in the Equatorial Pacific Ocean. This study revealed stereoscopic temperature factors for the prediction of tuna fishing ground. Maximal catches were observed in the fishing locations where (1) vertically there has a strong subsurface temperature front in the 150–200 m depth layer, with horizontal temperature gradient up to near 0.020 °C/km; (2) there have vertical temperature gradients between −0.088 and −0.066 °C/m.

Ocean temperature plays an important role in influencing the distribution of bigeye tuna fishery ground as the change of ocean temperature can cause many changes of marine biological and physical properties. In bigeye tuna fishing ground prediction, the following parameters should be considered first: horizontal temperature gradient, vertical temperature gradient in the 100–300 m layer, and then the 20 °C isotherm depth.

Other factors, such as SSH, the bigeye tuna's body size or the age of bigeye tuna and the seasonal or annual change of marine environmental factors can also be helpful in bigeye tuna fishing ground forecasting.

Acknowledgements

This work is jointly supported by the following research projects: The Planning Program of Science and Technology of Zhoushan (2016C41018); Guangdong Key Laboratory of Ocean Remote Sensing (South China Sea Institute of Oceanology Chinese Academy of Sciences) (2017B030301005-LORS2001), State Key Laboratory of Tropical Oceanography, South China Sea Institute of Oceanology, Chinese Academy of Sciences (Project No. LTO1609); Research Project of Zhejiang Department of Education (Y201840279); National Key Research and Development Program of China (2016YFC1401407); Comprehensive Risk Study of Global Change in Coastal Zones and Coastal Areas (2017YFA0604901). National Key Research and Development Program of China (2016YFC1401605). The open Foundation from Marine Sciences in the First-Class Subjects of Zhejiang Province (11104060218). The TAO/TRITON moored buoy data were obtained from http://www.pmel.noaa.gov/tao/data_deliv/frames/main.html.

References

Abascala, F.J., Peatmanb, T., Leroyb, B., Nicolc, S., Schaeferd, K., Fullerd, D.W., Hamptonb, J., 2018. Spatiotemporal variability in bigeye vertical distribution in the Pacific Ocean. Fish. Res. 204 (2018), 371–379. https://doi.org/10.1016/j.fishres.2018.03.013.

Anand, A., Kumari, B., Nayak, S.R., Krishnamurthy, Y.V.N., 2005. Locating oceanic tuna resources in the eastern Arabian sea using remote sensing. J. Indian Soc. Remote Sens. 33 (4), 511–520. https://doi.org/10.1007/BF02990736.

Belkin, I.M., Cornillon, P.C., Sherman, K., 2009. Fronts in large marine ecosystems. Progress Oceanography 81 (1-4), 223–236. https://doi.org/10.1016/j.pocean.2009.04.01.

Bertrand, A., Josse, E., Bach, P., Gros, P., Dagorn, L., 2002. Hydrological and trophic characteristics of tuna habitat: consequences on tuna distribution and longline catch ability. Can. J. Fish. Aquat. Sci. 59 (6), 1002–1013. https://doi.org/10.1139/F02-073.

Brill, R.W., Dewar, H., Graham, J.B., 1994. Basic concepts relevant to heat transfer in fishes, and their use in measuring the physiological thermoregulatory abilities of tunas. Environ. Biol. Fishes 40 (2), 109–124. https://doi.org/10.1007/bf00002538.

Chiang, H.C., Hsu, C.C., Wu, C.C., Chang, S.K., Yang, H.Y., 2008. Population structure of bigeye tuna (*Thunnus obesus*) in the Indian Ocean inferred from mitochondrial DNA. Fish. Res. 90 (1), 305–312. https://doi.org/10.1016/j.fishres.2007.11.006.

Cravatte, S., Kestenare, E., Marin, F., Dutrieux, P., Firing, E., 2017. Subthermocline and intermediate zonal currents in the tropical pacific ocean: paths and vertical structure. J. Phys. Oceanogr. 47. https://doi.org/10.1175/JPO-D-17-0043.1.

Dagorn, L., Bach, P., Josse, E., 2000. Movement patterns of large bigeye tuna (*Thunnus obesus*) in the open ocean, determined using ultrasonic telemetry. Mar. Biol. 136 (2), 361–371. https://doi.org/10.1007/s002270050694.

Evans, K., Langley, A., Clear, N.P., Williams, P., Gunn, J.S., 2008. Behavior and habitat preferences of bigeye tuna (obesus) and their influence on longline fishery catches in the western Coral Sea. Can. J. Fish. Aquat. Sci. 65, 2427–2443. https://doi.org/10.1139/F08-148.

Evans, K., Lea, M.A., Patterson, T.A., 2013. Recent advances in bio-logging science: Technologies and methods for understanding animal behaviour and physiology and their environments. Deep Sea Res. Part II 88–89, 1–6. https://doi.org/10.1016/j.dsr2.2012.10.005.

Fan, W., Chen, X., Cui, X., 2008. Study on the Relationship of Longline Bigeye Tuna and SST in the Pacific Ocean. Marine Sci. Bull. 27 (1), 35–41. https://doi.org/10.1007/s11676-008-0012-9.

Fuller, D., Schaefer, K., Hampton, J., Caillot, S., Leroy, B., Itano, D., 2015. Vertical movements, behavior, and habitat of bigeye tuna (*Thunnus obesus*) in the equatorial central Pacific Ocean. Fish. Res. 172, 57–70. https://doi.org/10.1016/j.fishres.2015.06.024.

Hino, H., Kitagawa, T., Matsumoto, T., Aoki, Y., Kimura, S., 2019. Changes to vertical thermoregulatory movements of juvenile bigeye tuna (*Thunnus obesus*) in the northwestern Pacific Ocean with time of day, seasonal ocean vertical thermal structure, and body size. Fisheries Oceanography. https://doi.org/10.1111/fog.12417.

Houssard, P., Lorrain, A., Tremblay-Boyer, L., Allain, Valerie, Graham, B.S., Menkes, C.E., 2017. Trophic position increases with thermocline depth in yellowfin and bigeye tuna across the Western and Central Pacific Ocean S007966111630177X. Prog. Oceanogr. https://doi.org/10.1016/j.pocean.2017.04.008.

Howell, E.A., Kobayashi, D.R., 2006. El Niño effects in the Palmyra Atoll region: oceanographic changes and bigeye tuna (*Thunnus obesus*) catch rate variability. Fish. Oceanogr. 15 (6), 477–489. https://doi.org/10.1111/j.1365-2419.2005.00397.x.

Howell, E.A., Hawn, D.R., Polovina, J.J., 2010. Spatiotemporal variability in bigeye tuna (*Thunnus obesus*) dive behavior in the central North Pacific Ocean. Prog. Oceanogr. 86 (1–2), 81–93. https://doi.org/10.1016/j.pocean.2010.04.013.

Jean-Rene, D., Meyers, Gary., 1987. Observed and modelled topography of the 20°C isotherm in the tropical. Pacific. Oceanologica Acta 10.

Lam, C.H., Galuardi, B., Lutcavage, M.E., 2014. Movements and oceanographic associations of bigeye tuna (*Thunnus obesus*) in the northwest. Atlantic. Can. J. Fisheries Aquatic Sci. 71 (10), 1529–1543. https://doi.org/10.1139/cjfas-2013-0511.

Laurs, R.M., Fiedler, P.C., Montgomery, D.R., 1984. Albacore tuna catch distributions relative to environmental features observed from satellites. Deep-Sea Res. 31 (9), 1085–1099. https://doi.org/10.1016/0198-0149(84)90014-1.

Lehodey, P., 1997. El Nino southern oscillation and tuna in the western Pacific. Nature 389 (6652), 715–718. https://doi.org/10.1038/39575.

Leroy, B., Itano, D., Nicol, S., 2007. Preliminary analysis and observations on the vertical behaviour of WCPO skipjack, yellowfin and bigeye tuna in association with anchored FADs, as indicated by acoustic and archival tagging data. Scientific Committee Third Regular Session, Honolulu, Hawaii, WCPFC-SC3-BI SW Thunnus G WP-4. https://doi.org/10.1007/978-1-4020-9640-2_10.

Li, Y., Song, L., Nishida, T., Gao, P., 2012. Development of integrated habitat indices for bigeye tuna, *Thunnus obesus*, in waters near Palau. Mar. Freshw. Res. 63 (12), 1244–1254. https://doi.org/10.1071/MF12072.

Liu, Y., Dong, C., Guan, Y., Chen, D., JamesMcWilliams, J., Nencioli, F., 2012. Eddy analysis in the subtropical zonal band of the North Pacific Ocean. Deep Sea Res. 68 (5), 54–67. https://doi.org/10.1016/j.dsr.2012.06.001.

Liu, D., Wang, Y., Wang, Y., Keesing, J.K., 2018. Ocean fronts construct spatial zonation in microfossil assemblages. Global Ecol. Biogeography 27 (10), 1225–1237. https://doi.org/10.1111/geb.12779.

Lumban-Gaol, J., Leben, R.R., Vignudelli, S., Mahapatra, K., Okada, Y., Nababan, B., et al., 2015. Variability of satellite-derived sea surface height anomaly, and its relationship with bigeye tuna (*Thunnus obesus*) catch in the eastern indian ocean. Eur. J. Remote Sens. 48 (48), 465–477.

Matsumoto, T., Kitagawa, T., Kimura, S., 2013. Vertical behavior of bigeye tuna (*Thunnus obesus*) in the northwestern Pacific Ocean based on archival tag data. Fish. Oceanogr. 22, 234–246. https://doi.org/10.1111/fog.12017.

Musyl, M.K., Brill, R.W., Boggs, C.H., Curran, D.S., Kazama, T.K., Seki, M.P., 2010. Vertical movements of bigeye tuna (*Thunnus obesus*) associated with islands, buoys, and seamounts near the main Hawaiian Islands from archival tagging data. Fish. Oceanogr. 12 (3), 152–169. https://doi.org/10.1046/j.1365-2419.2003.00229.x.

Mysak, L.A., 1986. El nino, interannual variability and fisheries in the northeast pacific ocean. Can. J. Fish. Aquat. Sci. 43 (2), 464–497.

Oliver, M.A., Webster, R., 1990. Kriging: a method of interpolation for geographical information systems. Int. J. Geographical Informat. Syst. 4 (3), 313–332. https://doi.org/10.1080/02693799008941549.

Song, L.M., Xu, L.X., Chen, X.J., 2004. Relationship between bigeye tuna vertical distribution and the temperature, salinity in the Central Atlantic Ocean. J. Fishery Sci. China 11 (6), 561–566.

Song, L.M., Zhao, H.L., Xie, K., Li, D.J., 2015. Effects of environmental variables on catch rates of *Thunnus obesus* in waters near Cook Islands. J. Fisheries China 39 (8), 1230–1241.

Song, L., Zhou, J., Zhou, Y., Nishida, T., Jiang, W., Wang, J., 2009. Environmental preferences of bigeye tuna, *Thunnus obesus*, in the Indian Ocean: an application to a longline fishery. Environ. Biol. Fishes 85 (2), 153–171. https://doi.org/10.1007/s10641-009-9474-7.

Song, L., Zhou, Y., 2010. Developing an integrated habitat index for bigeye tuna (*Thunnus obesus*) in the Indian Ocean based on longline fisheries data. Fish. Res. 105 (2), 63–74. https://doi.org/10.1016/j.fishres.2010.03.004.

Sun, W., Dong, C., Wang, R., Liu, Y., Yu, K., 2017. Vertical structure anomalies of oceanic eddies in the Kuroshio Extension region. J. Geophys. Res. 122 (2), 1476–1496. https://doi.org/10.1002/2016JC012226.

Sun, W., Dong, C., Tan, W., Liu, Y., He, Y., Wang, J., 2018. Vertical structure anomalies of oceanic eddies and eddy-induced transports in the South China Sea. Remote Sens. 10 (795). https://doi.org/10.3390/rs10050795.

Syamsuddin, M., Saitoh, S.I., Hirawake, T., Syamsudin, F., Zainuddin, M., 2016. Interannual variation of bigeye tuna (*Thunnus obesus*) hotspots in the eastern Indian ocean off java. Int. J. Remote Sens., 1–14

Wang, Q., Hu, D., 2006. Bifurcation of the north equatorial current derived from altimetry in the Pacific Ocean. J. Hydrodyn. 18 (5), 620–626. https://doi.org/10.1016/s1001-6058(06)60144-3.

Yang, S., Ma, J., Wu, Y., Fan, X., Jin, S., Chen, X., 2015. Relationship between temporal–spatial distribution of fishing grounds of bigeye tuna (*Thunnus obesus*) and thermocline characteristics in the Atlantic Ocean. Acta Ecol. Sinica 35. https://doi.org/10.1016/j.chnaes.2014.07.005.

Zagaglia, C.R., Lorenzzetti, J.A., Stech, J.L., 2004. Remote sensing data and longline catches of yellowfin tuna (Thunnus albacares) in the equatorial Atlantic. Remote Sens. Environ. 93 (1/2), 267–281. https://doi.org/10.1016/j.rse.2004.07.015.

Please cite this article as: L. Cai, L. Xu, D. Tang et al., The effects of ocean temperature gradients on bigeye tuna (*Thunnus obesus*) distribution in the equatorial eastern Pacific Ocean, Advances in Space Research, https://doi.org/10.1016/j.asr.2020.03.030